Citation for published version:

Xiaojing Chen, Wei Ni, Xin Wang, Yichuang Sun, "Optimal Quality-of-Service Scheduling for Energy-Harvesting Powered Wireless Communications", *IEEE Transactions on Wireless Communications,* Vol. 15 (5): 3269-3280, January 2016.

DOI:

10.1109/TWC.2016.2519411

Optimal Quality-of-Service Scheduling for Energy-Harvesting Powered Wireless Communications

Xiaojing Chen, *Student Member, IEEE*, Wei Ni, *Senior Member, IEEE*, Xin Wang, *Senior Member, IEEE*, and Yichuang Sun, *Senior Member, IEEE*

***Abstract*—In this paper, a new "dynamic string tautening" algorithm is proposed to generate the most energy-efficient off-line schedule for delay-limited traffic of transmitters with non-negligible circuit power. The algorithm is based on two key findings that we derive through judicious convex formulation and resultant optimality conditions, specifies a set of simple but optimal rules, and generates the optimal schedule with a low complexity of $\mathcal{O}(N^2)$ in the worst case. The proposed algorithm is also extended to on-line scenarios, where the transmit schedule is generated on-the-fly. Simulation shows that the proposed algorithm requires substantially lower average complexity by almost two orders of magnitude to retain optimality than general convex solvers. The effective transmit region, specified by the trade-off of the data arrival rate and the energy harvesting rate, is substantially larger using our algorithm than using other existing alternatives. Significantly more data or less energy can be supported in the proposed algorithm.**

***Index Terms*—Energy harvesting; convex optimization; non-ideal circuit power.**

I. Introduction

Energy harvesting (EH) is a process of capturing and converting ambient energy (e.g., solar, wind and thermal energy) into usable electrical energy [1]. In wireless communication systems, environmental EH is a critical component to build self-sustainable networks, such as wireless sensor networks in remote human-unfriendly environments [2]. On the other hand, Quality-of-Service (QoS), such as delay and packet error rate, is crucial to many wireless applications [2], [3]. Many sensory data are delay intolerant, especially in bushfire or flood monitoring, and security/safety surveillance applications.

Three critical challenges arise in providing QoS to EH powered wireless transmissions. The first critical challenge is to generate QoS-guaranteed transmit schedules, given the unreliable and unstable power supply of EH. The harvested energy is time-varying. It can become insufficient to transmit data by their deadlines, if the transmissions are inadequately scheduled. The second critical challenge is to increase the energy efficiency (EE) of transmissions, especially in short-range wireless sensor networks where the energy consumed on the circuits (e.g., signal processing, digital-to-analogue conversion, and power amplification) is non-negligible [4]. It is important to make the insufficient energy meet the transmission requirement, reducing outage probability and QoS violations. The third critical challenge of providing QoS to EH powered transmissions is to reduce the computational complexity of generating schedules and in turn the energy consumption [2]. General convex optimization solvers (such as interior point methods [5]) may not be computationally efficient to solve this specific problem. Developing low-complexity specialized solvers may be required.

Some recent works have been conducted in EH powered wireless systems [6]–[13], but none of them addresses the three challenges of QoS provision, energy efficiency, and computational complexity, altogether. The works [6]–[13] were all focused on delay-tolerant traffic, thus cannot provide QoS to delay-intolerant applications in practical systems. In [6], [7], the optimal schedules were generated to maximize the delay-tolerant throughput of an EH powered wireless link with negligible circuit power in time-invariant channels. In [8], a directional water-filling approach was proposed to maximize the throughput in time-varying channels. In [9], an "on-off" transmit schedule was developed to maximize the throughput of delay-tolerant traffic over a static point-to-point channel with non-ideal circuit power consumption. Later, extensions to time-varying channels were carried out in [10], [11]. Asymptotically optimal resource allocation was developed to maximize the throughput of delay-tolerant traffic for EH point-to-point link, where symbols could be transmitted through several parallel independent streams in [12]. In [13], a game theoretic approach was proposed to distribute the EH power of a relay among multiple source-destination pairs, which improved the trade-off between the outage of delay-tolerant traffic and system complexity for wireless cooperative networks.

In a different context from our paper, there are recent works focused on energy efficient transmissions of delay-sensitive traffic in systems with persistent power supply, such as [14], [15]. In [14], a "string tautening" algorithm was proposed to produce the most energy-efficient schedule for

Manuscript submitted May 8, 2015; revised September 30, 2015 and November 30, 2015; accepted January 12, 2016. Work in this paper is supported by the the China Recruitment Program of Global Young Experts, the Program for New Century Excellent Talents in University, the Innovation Program of Shanghai Municipal Education Commission.

X. Chen and X. Wang are with the Key Laboratory for Information Science of Electromagnetic Waves (MoE), Dept. of Communication Science and Engineering, Fudan University, 220 Han Dan Road, Shanghai, China, email: xwang11@fudan.edu.cn; X. Wang is also with the Dept. of Computer & Electrical Engineering and Computer Science, Florida Atlantic University, 777 Glades Road, Boca Raton, FL 33431.

W. Ni is with the Digital Productivity and Service (DP&S) Flagship, CSIRO, Sydney, Australia, NSW 2122.

Y. Sun is with the School of Engineering and Technology, University of Hertfordshire, Hatfield AL10 9AB, UK.

delay-limited traffic, where the circuit power was assumed to be negligible. Given the persistent and sufficient power supply, the optimal schedule was generated by tautening a string between the static staircase curves of the data amount that can be transmitted by any instant and that must be transmitted by then. In [15], the algorithm was extended to the case of non-negligible circuit power. However, it is non-trivial to extend these string tautening algorithms to EH systems, where unreliable and insufficient power supply can stop the data which are due from being transmitted (as is never experienced with persistent power supplies). Transmissions powered by EH also undergo dependence among the data amount transmitted across the schedule. Every instant a transmit rate is decided, the remaining (insufficient) energy for the rest of the schedule can change, and so do the data that can be transmitted at future instants. None of the existing string tautening algorithms can deal with the dependence. More works also include [16]–[19], which assumed persistent power supplies and cannot apply to EH powered systems.

In this paper, we propose a new Dynamic String Tautening (DST) algorithm, which jointly addresses the three critical challenges altogether and generates the most energy-efficient off-line schedule for delay-limited traffic of transmitters with non-negligible circuit power. While [6]–[13] aimed to maximize the throughput of delay-tolerant traffic under the assumption that data were always available, here we consider the EH powered transmission of delay-sensitive packets that arrive in bursts and need to be delivered before strict deadlines. Our algorithm is based on two key findings that we derive through judicious convex formulation and resultant optimality conditions. The findings are visualized and interpreted as a set of rules which guide us to generate the optimal schedule in a computationally efficient, graphical manner by tautening a transmit string in a recursively updated solution region. The optimal transmit schedule here can be produced with a low computational complexity (which is $\mathcal{O}(N^2)$ in the worst case, where N is the number of instants within a schedule).

Given the optimality and reduced complexity of the algorithm, we further extend it to on-line scenarios, where the transmit schedule is generated on-the-fly. Simulation results show that our proposed algorithm requires substantially lower average complexity (i.e., less energy) to retain optimality than the standard convex programming methods, reducing the CPU running time by almost two orders of magnitude. As a result, the effective transmit region, specified by the data arrival rate and the EH rate, is substantially larger using our algorithm than using general convex solvers. In other words, significantly more data or less energy can be supported in the proposed algorithm.

In our earlier work [20], the transmit schedule was optimized for delay-limited traffic of EH powered links with negligible circuit power. The new algorithm proposed in this paper is substantially different, because the consideration of non-ideal circuit power consumption results in a different optimization problem and hence the distinct structure of the optimal schedule. When compared to the proposed algorithm, a significant loss of data and energy efficiency could occur when the schedule generated in [20] is applied in the case of non-ideal circuit power consumption (as will be shown in Section VI). In [21], we gave a brief introduction on the concept of the new algorithm without providing technical details. In this paper, the full technical details are provided, and the optimality is rigorously proved. Moreover, the paper also extends the algorithm to generate the on-line transmit schedule on-the-fly.

The main contributions of the paper can be summarized as follows:

(a) the consideration of the new scenario of EH powered transmission of data packets with strict deadlines, where the new challenge of unreliable power supply is imposed;

(b) a new DST algorithm to generate the optimal transmit schedule in a computationally efficient, graphical manner by recursively updating the energy constraint curve on-the-go;

(c) a well-structured on-line algorithm, which follows the optimal rules that we develop, and produces the transmit schedule in real-time without a-priori knowledge on the data or energy arrivals.

The rest of the paper is organized as follows. In Section II, the system model is described. In Section III, the convex optimization problem is formulated and the two key insightful findings are derived. In Section IV, the proposed DST algorithm is elaborated on, which produces the optimal off-line schedule for delay-sensitive bursty data. In Section V, the proposed algorithm is extended to practical on-line scenarios. In Section VI, simulations are carried out to validate the optimality of our algorithm and its superiority of reduced complexity, followed by conclusions in Section VII.

II. System Model

Consider a time-invariant wireless link, where the transmitter is powered by EH. Let $E_{\max}$ denote the capacity of the rechargeable battery at the transmitter. The channel coefficient of the wireless link is denoted by h, and the transmit rate of the link is r. The additive white Gaussian noise (AWGN) is assumed to have unit variance at the receiver.

Our discussion is focused on a time period $[0, T]$, over which there are $(N+1)$ time instants: $0 = t_0 < t_1 < t_2 < \cdots < t_N = T$. We refer to the interval between two consecutive time instants as an *epoch*; the duration of the ith epoch is $L_i = t_i - t_{i-1}$, $i = 1, \cdots, N$.

At each time instant $t_i\,(i = 0, 1, \cdots, N)$, new energy is harvested, or new bursty data are collected, or strict deadlines of the collected data are reached at the transmitter. The amount of the harvested energy, the collected data, and the data whose deadlines are reached can be written respectively as sequences $\{E_0, E_1, E_2, \cdots, E_{N-1}, 0\}$, $\{A_0, A_1, A_2, \cdots, A_{N-1}, 0\}$, and $\{0, D_1, D_2, \cdots, D_{N-1}, D_N\}$, corresponding to the time instants $\{t_0, t_1, t_2, \cdots, t_{N-1}, t_N\}$. $E_i \geq 0$ is the energy harvested at t_i; $A_i \geq 0$ is the number of packets collected at t_i; $D_i \geq 0$ is the number of packets that must be transmitted by t_i. E_0 and A_0 are the initial energy level and the initial number of packets at the transmitter. Note that we consider the optimal schedule for the general case where the packets can have different delay requirements, i.e., the packets are of different traffic types or for different applications. Whenever new packets arrive, the transmitter may need to re-shuffle the packets in the buffer to ensure that the packets with more stringent deadlines are placed head-of-line. For the special case that all the packets have the same delay requirements, such reshuffling becomes unnecessary and the data queue simply operates in a first-in-first-out manner.

We set $E_N = A_N = 0$, as any energy harvested or data collected at t_N cannot be dealt with during the current time period of $[0, T]$ and will be used to initialize the next time period. Also, it is clear that $\sum_{i=0}^{N-1} A_i = \sum_{i=1}^{N} D_i$. In other words, the total number of packets required to deliver is equal to that of arrived packets.

III. Convex Formulation and Resultant Optimality Conditions

In this section, we mathematically characterize the optimal transmit schedule under the ideal (impractical) assumption that the arrival processes of data and energy are known a priori to the transmitter. The variables l_i and r_i ($i = 1, \cdots, N$) are to be optimized, where $l_i \in [0, L_i]$ is the duration that the transmitter is on during epoch i and r_i is the transmit rate associated with l_i.

The way of our interpreting the optimal schedule is new. It involves formulating the convex optimization problem and rigorously proving that the optimal solution can be directly constructed based on the resultant optimality conditions. This lays foundation to a new simple and efficient on-line scheduling algorithm in practical scenarios where the data arrivals and energy collections are unknown a priori, as will be described in Sections IV and V.

First, the total power P_{total} consumed by the transmitter can be given by [9], [16]:

$$P_{total} = \begin{cases} \frac{P}{\eta} + \rho, & P > 0, \\ \beta, & P = 0, \end{cases} \tag{1}$$

where ρ denotes the circuit power consumption when the transmitter is transmitting (i.e., in an "on" mode), β the circuit power consumption when the transmitter is idle (i.e., in an "off" mode) and η the efficiency of the RF chain at the transmitter. For specificity, the transmit power P is given by

$$P(r) = \frac{1}{|h|^2}(e^r - 1), \tag{2}$$

where r is the instantaneous data rate of the wireless link.[1] We assume $\rho > 0$ and $\beta = 0$ without loss of generality, since $\rho \gg \beta$ in practical systems [16]. We also assume $\eta = 1$, as η is just a scaling factor.

Given that $P(r)$ is convex, it was proved that the transmit rate over the "on" period l_i of each epoch i, r_i, should remain unchanged in the optimal schedule [9]. The problem of interest becomes to find the optimal pairs of (r_i, l_i), $i = 1, \cdots, N$, to minimize the total energy consumed to deliver data packets by their deadlines. The problem can be formulated as

$$\begin{aligned} \min_{\boldsymbol{r}, \boldsymbol{l}} \quad & \sum_{i=1}^{N} \{[P(r_i) + \rho] l_i\} \\ \text{s.t.} \quad & r_i \geq 0, \quad 0 \leq l_i \leq L_i, \ \ \forall i; \\ & (\mathbf{C1}): \ \sum_{i=1}^{n} (r_i l_i) \leq \sum_{i=0}^{n-1} A_i; \\ & (\mathbf{C2}): \ \sum_{i=1}^{n} (r_i l_i) \geq \sum_{i=1}^{n} D_i; \\ & (\mathbf{C3}): \ \sum_{i=1}^{n} \{[P(r_i) + \rho] l_i\} \leq \sum_{i=0}^{n-1} E_i; \\ & (n = 1, \cdots, N), \end{aligned} \tag{3}$$

where $\boldsymbol{r} := \{r_1, r_2, \dots, r_N\}$ collects the transmit rates during the "on" periods of the epochs, and $\boldsymbol{l} := \{l_1, l_2, \dots, l_N\}$ collects the durations of the "on" periods of the epochs.

Here, (**C1**) presents the data causality constraints: the number of packets $\sum_{i=1}^{n}(r_i l_i)$ transmitted up to any time t_n cannot exceed the number of available packets $\sum_{i=0}^{n-1} A_i$ at the transmitter's buffer. (**C2**) presents the deadline constraints: $\sum_{i=1}^{n}(r_i l_i)$ must be no less than the data required to be transmitted to meet their deadlines, i.e., $\sum_{i=1}^{n} D_i$. (**C3**) presents the energy causality constraints: the total amount of energy $\sum_{i=1}^{n} \{[P(r_i) + \rho] l_i\}$ consumed up to any time t_n must be no greater than $\sum_{i=0}^{n-1} E_i$ that has been harvested and accumulated in the battery so far.

Clearly, (3) is not convex or concave, because neither of $r_i l_i$ and $P(r_i) l_i$ is convex or concave with respect to (r_i, l_i). Yet, it can be reformulated into a convex program through a series of changes of variables. Define $\Phi_i := r_i l_i$ and $\boldsymbol{\Phi} := \{\Phi_1, \Phi_2, \dots, \Phi_N\}$. We can rewrite (3) into

$$\begin{aligned} \min_{\boldsymbol{\Phi}, \boldsymbol{l}} \quad & \sum_{i=1}^{N} \{[P(\frac{\Phi_i}{l_i}) + \rho] l_i\} \\ \text{s.t.} \quad & \Phi_i \geq 0, \quad 0 \leq l_i \leq L_i, \ \ \forall i, \\ & \sum_{i=1}^{n} \Phi_i \leq \sum_{i=0}^{n-1} A_i, \\ & \sum_{i=1}^{n} \Phi_i \geq \sum_{i=1}^{n} D_i, \\ & \sum_{i=1}^{n} \{[P(\frac{\Phi_i}{l_i}) + \rho] l_i\} \leq \sum_{i=0}^{n-1} E_i; \\ & (n = 1, \cdots, N). \end{aligned} \tag{4}$$

where we have $P(\frac{\Phi_i}{l_i}) l_i = 0$ if $l_i = 0$. For any convex $P(r_i)$, $P(\frac{\Phi_i}{l_i}) l_i$ is called its perspective, and is a convex function of (Φ_i, l_i) [22]. As a result, (4) is a convex problem.

Let $\boldsymbol{\Lambda} := \{\lambda_n^c, \lambda_n^d, \mu_n^c, n = 1, \dots, N\}$ where λ_n^c, λ_n^d, and μ_n^c are the Lagrange multipliers associated with the data causality, deadline and energy causality constraints, respec-

[1] The proposed approach applies to any other convex power functions.

tively. The Lagrangian of (4) is given by

$$
\begin{aligned}
L(\boldsymbol{r},\boldsymbol{l},\boldsymbol{\Lambda}) = & \sum_{i=1}^{N}\{[P(\frac{\Phi_i}{l_i})+\rho]l_i\} + \sum_{n=1}^{N}\lambda_n^c(\sum_{i=1}^{n}\Phi_i - \sum_{i=0}^{n-1}A_i) \\
& + \sum_{n=1}^{N}\lambda_n^d(\sum_{i=1}^{n}D_i - \sum_{i=1}^{n}\Phi_i) \\
& + \sum_{n=1}^{N}\mu_n^c\{\sum_{i=1}^{n}\{[P(\frac{\Phi_i}{l_i})+\rho]l_i\} - \sum_{i=0}^{n-1}E_i\} \\
= & C(\boldsymbol{\Lambda}) + \sum_{i=1}^{N}\{\{[P(\frac{\Phi_i}{l_i})+\rho]l_i\}(1+\sum_{n=i}^{N}\mu_n^c) \\
& - \Phi_i(\sum_{n=i}^{N}\lambda_n^d - \sum_{n=i}^{N}\lambda_n^c)\},
\end{aligned}
$$

where $C(\boldsymbol{\Lambda}) := -\sum_{n=1}^{N}\lambda_n^c(\sum_{i=0}^{n-1}A_i) + \sum_{n=1}^{N}\lambda_n^d \times (\sum_{i=1}^{n}D_i) - \sum_{n=1}^{N}\mu_n^c(\sum_{i=0}^{n-1}E_i)$ for notation simplicity.

Let $(\boldsymbol{\Phi^*},\boldsymbol{l^*})$ denote the optimal solution for (4), and $\boldsymbol{\Lambda^*}$ the optimal Lagrange multiplier vector for its dual problem. Also define per epoch i:

$$w_i := \sum_{n=i}^{N}[(\lambda_n^d)^* - (\lambda_n^c)^*]/[1+\sum_{n=i}^{N}(\mu_n^c)^*]. \tag{5}$$

Then the sufficient and necessary Karush-Kuhn-Tucker (KKT) optimality conditions for (4) dictate that [23]: $\forall i$,

$$(\Phi_i^*, l_i^*) = \arg\min_{\Phi_i\geq 0,\, 0\leq l_i\leq L_i}\{[P(\frac{\Phi_i}{l_i})+\rho]l_i - w_i\Phi_i\}; \tag{6}$$

and the non-negative $(\lambda_n^c)^*$, $(\lambda_n^d)^*$ and $(\mu_n^c)^*$ satisfy the complementary slackness conditions: $\forall n$,

$$\begin{cases} (\lambda_n^c)^* = 0, \quad \text{if } \sum_{i=1}^{n}\Phi_i^* < \sum_{i=0}^{n-1}A_i; \\ \sum_{i=1}^{n}\Phi_i^* = \sum_{i=0}^{n-1}A_i, \quad \text{if } (\lambda_n^c)^* > 0; \end{cases} \tag{7}$$

$$\begin{cases} (\lambda_n^d)^* = 0, \quad \text{if } \sum_{i=1}^{n}\Phi_i^* > \sum_{i=1}^{n}D_i; \\ \sum_{i=1}^{n}\Phi_i^* = \sum_{i=1}^{n}D_i, \quad \text{if } (\lambda_n^d)^* > 0; \end{cases} \tag{8}$$

$$\begin{cases} (\mu_n^c)^* = 0, \quad \text{if } \sum_{i=1}^{n}\{[P(\frac{\Phi_i}{l_i})+\rho]l_i\} < \sum_{i=0}^{n-1}E_i; \\ \sum_{i=1}^{n}\{[P(\frac{\Phi_i}{l_i})+\rho]l_i\} = \sum_{i=0}^{n-1}E_i, \quad \text{if } (\mu_n^c)^* > 0. \end{cases} \tag{9}$$

For any i, we let $r_i^* = \frac{\Phi_i^*}{l_i^*}$ if $l_i^* > 0$, and allow r_i^* to take an arbitrary non-negative value if $l_i^* = 0$. It is obvious that $(\boldsymbol{r}^*,\boldsymbol{l}^*)$ is the optimal solution to (3).

From (6)–(9), we can establish the sufficient and necessary optimality conditions for (3), as given by

$$(r_i^*, l_i^*) = \arg\min_{r_i\geq 0,\, 0\leq l_i\leq L_i}[P(r_i)+\rho - w_i r_i]l_i \tag{10}$$

$$\begin{cases} (\lambda_n^c)^* = 0, \quad \text{if } \sum_{i=1}^{n}(r_i l_i) < \sum_{i=0}^{n-1}A_i, \\ \sum_{i=1}^{n}(r_i l_i) = \sum_{i=0}^{n-1}A_i, \quad \text{if } (\lambda_n^c)^* > 0; \end{cases} \tag{11}$$

$$\begin{cases} (\lambda_n^d)^* = 0, \quad \text{if } \sum_{i=1}^{n}(r_i l_i) > \sum_{i=1}^{n}D_i, \\ \sum_{i=1}^{n}(r_i l_i) = \sum_{i=1}^{n}D_i, \quad \text{if } (\lambda_n^d)^* > 0; \end{cases} \tag{12}$$

$$\begin{cases} (\mu_n^c)^* = 0, \text{ if } \sum_{i=1}^{n}\{[P(r_i)+\rho]l_i\} < \sum_{i=0}^{n-1}E_i, \\ \sum_{i=1}^{n}\{[P(r_i)+\rho]l_i\} = \sum_{i=0}^{n-1}E_i, \text{ if } (\mu_n^c)^* > 0. \end{cases} \tag{13}$$

For any given $l_i > 0$, from (10) we can have the optimal transmit rate r_i^*, as given by

$$r_i^* = \arg\min_{r_i\geq 0}\ [P(r_i)+\rho - w_i r_i]. \tag{14}$$

As $P(r_i)$ is strictly convex and increasing, this is equivalent to: $P'(r_i^*) = w_i$, where $P'(\cdot)$ denotes the first derivative of function $P(\cdot)$.

Substituting $P'(r_i^*) = w_i$ into (10), we can have

$$l_i^* = \arg\min_{0\leq l_i\leq L_i}\ [P(r_i^*)+\rho - P'(r_i^*)r_i^*]l_i, \tag{15}$$

which is the optimal duration of the "on" period per epoch i.

The followings are two key findings derived from (14) and (15).

Lemma 1. *The optimal schedule for (3) can only adopt one of the following three strategies per epoch i: (i) $l_i^* = 0$ (i.e., "off"), (ii) $r_i^* = r_{ee}$ and $l_i^* \leq L_i$ (i.e., "first-on-then-off" or "on-off" for short), or (iii) $r_i^* > r_{ee}$ and $l_i^* = L_i$ (i.e., "on"). Specifically, r_{ee} is the bits-per-Joule EE-maximizing rate, i.e.,*

$$r_{ee} = \arg\max_{r\geq 0}\frac{r}{P(r)+\rho}, \tag{16}$$

and can be efficiently obtained through a bisectional search [9], because $\frac{r}{P(r)+\rho}$ is (concave-over-linear) quasi-concave.

Proof: See Appendix A. ■

Lemma 1 shows that any transmit rate $r_i < r_{ee}$ should not be adopted in the optimal schedule. In fact, since r_{ee} maximizes the bits-per-Joule EE, a transmission strategy with an $r_i < r_{ee}$ over an epoch is always dominated by an on-off transmission with r_{ee}, which can use less energy to deliver the same data amount. Only when the data deadlines are strict (i.e., no further delay is allowed) should we adopt an $r_i^* > r_{ee}$; in this case, the transmitter should be always on, i.e., $l_i^* = L_i$, over epoch i.

Let $P'^{-1}(\cdot)$ denote the inverse function of $P'(\cdot)$. If $l_i^* > 0$, we can obtain from (14) that

$$
\begin{aligned}
r_i^* &= \arg\min_{r_i\geq 0}[P(r_i)+\rho - w_i r_i] := P'^{-1}(w_i) \\
&= \log(|h|^2 w_i)
\end{aligned} \tag{17}
$$

which is an increasing function of w_i.

Given (17) and (11)–(13), we establish the following structure of the optimal transmit schedule, as stated in Lemma 2.

Lemma 2. *In the optimal schedule for* (3)*, the transmit rate r_i^* only changes at t_n on which the data causality, deadline or energy causality constraints are met with equality. Specifically, r_i^* increases after t_n with $\sum_{i=1}^{n}(r_i^* l_i^*) = \sum_{i=0}^{n-1}A_i$ or $\sum_{i=1}^{n}\{[P(r_i^*)+\rho]l_i^*\} = \sum_{i=0}^{n-1}E_i$, and decreases after t_n with $\sum_{i=1}^{n}(r_i^* l_i^*) = \sum_{i=1}^{n}D_i$.*

Proof: See Appendix B. ■

Lemma 2 shows that the optimal transmit rate of the EH powered transmitter changes, if and only if the constraints take effect. Otherwise, the transmit rate should be maintained constant to minimize the energy consumption.

Note that this optimal off-line schedule could be obtained using standard convex programming methods. However, general convex solvers (e.g., the interior point methods) would

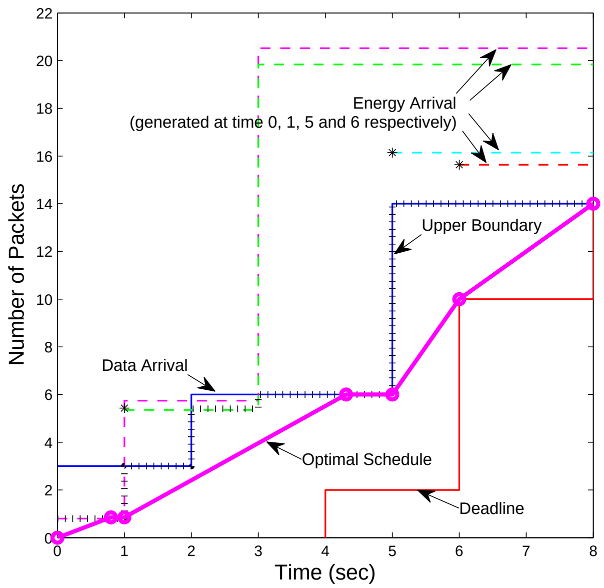

Fig. 1. An illustrative example of the proposed DST method and the achieved optimal transmission schedule.

require much higher complexity, which, in turn, compromises the optimality of the schedule by increasing power consumption on the circuit. Details will be provided in Section VI. In addition, no key findings would be observed to guide the design of practical on-line scheduling, if a standard convex programming solver is adopted.

IV. Proposed Optimal Off-line Dynamic String Tautening Algorithm

In this section, we propose a new DST algorithm, which produces the optimal schedule for delay-sensitive data over EH powered wireless links, given the a-priori knowledge on E_i, A_i and D_i $(i = 0, \cdots, N)$. Based on the key results of the mathematical characterization in Section III, the algorithm provides the energy consumption lower bound for EH powered wireless links. It will also be extended to play a key role in practical on-line operations where the a-priori knowledge is absent, as will be described in Section V.

A. Visualization of Dynamic String Tautening

Fig. 1 illustrates our proposed DST process, where the data arrival curve $A_d(t)$ plots the amount of data generated for transmission and the deadline (minimum data departure) curve $D_{\min}(t)$ plots the amount of data reaching their deadlines. $A_d(t)$ and $D_{\min}(t)$ can be written as

$$A_d(t) = \sum_{i=0}^{N-1} [A_i u(t - t_i)], \qquad (18)$$

$$D_{\min}(t) = \sum_{i=1}^{N} [D_i u(t - t_i)], \qquad (19)$$

where $0 \le t \le T$ and $u(t)$ is the unit-step function. $A_d(t)$ and $D_{\min}(t)$ are plotted in the very beginning and fixed, prior to the string tautening process, similar to the existing string tautening algorithm [17].

There are a series of energy curves, sequentially produced from left to right. Each curve plots the maximum amount of data that can be transmitted at future instants, given both the energy harvested and the data transmitted so far. The energy curves are plotted as follows.

At an instant t_τ where the transmit rate changes, a new energy curve starting from t_τ is generated tentatively by assuming that the transmitter remains "on" over all the remaining unscheduled epochs, as given by

$$A_{e_\tau}(t) = \sum_{i=\tau}^{N-1} \Big[(r^e_{i+1} \sum_{n=\tau+1}^{i+1} L_n - r^e_i \sum_{n=\tau+1}^{i} L_n) u(t - t_i) \Big], \qquad (20)$$

where $r^e_i > 0$ satisfies $\sum_{k=\tau+1}^{i} \{[P(r^e_i) + \rho] L_k\} = \sum_{k=\tau}^{i-1} e_k$, or $r^e_i = 0$, with e_τ being the residual energy in the battery by instant t_τ, and $e_k = E_k$ for $k = \tau + 1, \cdots, N$.

The $A_{e_\tau}(t)$ curve of (20) may not be exact, as the optimal transmit rate $r^*_{\tau+1}$ that is yet to be determined for the epoch beginning at t_τ may differ from $r^e_{\tau+1}$. The curve may need to be adjusted once the optimal transmit rate is determined; and in turn, it can affect the duration of the transmission with the optimal rate. Details will be provided later.

The $A_d(t)$, $D_{\min}(t)$, and $A_{e_\tau}(t)$ curves specify the (tentative) closed feasible solution region for the transmit rate. Specifically, the $A_d(t)$ and $A_{e_\tau}(t)$ curves provide the upper boundary of the region, and the $D_{\min}(t)$ curve provides the lower boundary, as shown in the figure.

We can generate the optimal data departure curve $D^*(t)$ whose slopes present the optimal transmit rates r^*_i, within the feasible solution region, yielding the following rules.

1) Connect the origin $(0, 0)$ and the rightmost joint of the $A_d(t)$ and $D_{\min}(t)$ curves with a string, and tauten the string tight so that it only bends at the corners.
2) Compare the slope of the lowest straight segment of the string to r_{ee}.
   a) If the slope is no less than r_{ee}, set the right end of the segment to be the left end of a new string.
   b) If the slope is less than r_{ee},
      i) shift the right end of the segment leftwards along the $A_d(t)$ or $A_{e_\tau}(t)$ curve, and tauten the segment until it intersects the $A_d(t)$ or $A_{e_\tau}(t)$ curve with the slope of r_{ee}. If the segment bends at a corner and becomes two segments, repeat 2b-i) on the lower of the two segments, until the lower segment is unbent.
      ii) Update the $A_{e_\tau}(t)$ curve for the case where the lowest unbent segment adopts the "on-off" mode (r_{ee} is adopted), and update the lowest segment accordingly (i.e., if the segment intersects the $A_{e_\tau}(t)$ curve, it needs to be updated to intersect the updated $A_{e_\tau}(t)$ curve).
      iii) Set the corner right to the lowest unbent segment to be the left end of a new string.
3) Tauten the new string to the rightmost joint of the $A_d(t)$ and $D_{\min}(t)$ curves, and repeat 2) on the lowest straight segment of the new string.

Rules 1 and 3 are designed to satisfy Lemma 2, because a string tautening process (as described in the rules) can guarantee that the slope of the string increases after the string bends around a corner of the upper boundary of the feasible solution region, and decreases after bending around the corner of the lower boundary; refer to instants 5 and 6 in Fig. 1.

Rule 2a is based on both Lemma 1 (that $r_i^* \geq r_{ee}$) and Lemma 2 (that the optimal transmit rate keeps unchanged, until the data/energy causality constraint is met with equality and the rate increases; or the deadline constraint is met with equality and the rate decreases). The rule is optimal because it is able to meet the constraints in the most energy efficient way. For the epochs with $\Phi = r_i^* L_i \geq r_{ee} L_i$, any "on-off" strategy (r_i, l_i) with $r_i > r_i^*$ and $r_i l_i = \Phi$ would only increase the energy consumption, since

$$[P(r_i) + \rho] l_i = \Phi \frac{P(r_i) + \rho}{r_i} > \Phi \frac{P(r_i^*) + \rho}{r_i^*}, \tag{21}$$

where the inequality is due to the fact that $\frac{P(r)+\rho}{r}$ is strictly increasing when $r \geq r_{ee}$. The examples of implementing the rule are the epochs $[5, 6]$ and $[6, 8]$ in the figure.

Rule 2b is based on Lemma 1 that $r_i^* = r_{ee}$ with $l_i^* \leq L_i$ is the most energy efficient. The optimality of the rule lies in the fact that the energy cost for transmission of data amount $\Phi = r_i L_i$ over epochs is minimized by a transmission with $r_{ee} \geq r_i$ over an "on" period of $l_i^* = \Phi / r_{ee} < L_i$, as shown in

$$\begin{aligned}[P(r_{ee}) + \rho] l_i^* = \frac{[P(r_{ee}) + \rho]\Phi}{r_{ee}} = \Phi \min_{r \geq 0} \frac{P(r) + \rho}{r} \\ = \min_{r l_i = \Phi} [P(r) + \rho] l_i.\end{aligned} \tag{22}$$

The examples of implementing the rule are the epochs $[0, 1]$ and $[1, 5]$.

In this sense, Rule 2 generates the optimal transmit rate over the epochs where the rate does not change. Rule 3 extrapolates Rule 2 to generate such optimal rates across the transmission period $[0, T]$, rendering the optimality of the entire transmit schedule generated. Particularly, Rule 2b specifies that the left end of a new string to be tautened corresponds to the case where the transmitter is running out of either data or energy (i.e., the data or energy causality constraint is met with equality). No causality remains between the past and the current tautening processes. Tautening the new string using Rule 3 does not invalidate the optimality of the transmit schedules generated so far by Rule 2.

The reason for tentatively plotting the $A_{e_\tau}(t)$ curve as (20) also becomes clear. It is because the optimal transmit rate determined by Rule 2 may lift the tentative $A_{e_\tau}(t)$ curve due to the improved energy efficiency (as compared to r_i^e). The optimal transmit rate will not be invalidated by the lifted $A_{e_\tau}(t)$ curve, if the segment associated with the rate intersects with the $A_d(t)$ or $D_{\min}(t)$ curve. The optimal transmit rate will also remain valid, if the segment intersects with the tentative $A_{e_\tau}(t)$ curve, since the optimal transmit rate is r_{ee} in this case (as specified in Rule 2). However, the duration of the segment can increase to intersect the lifted $A_{e_\tau}(t)$ curve (or the $A_d(t)$ curve if the intersecting part of the $A_d(t)$ curve is between the tentative and lifted $A_{e_\tau}(t)$ curves). An example is given by epoch $[0, 1]$ in the figure, where l_1^* is slightly extended to intersect the lifted (pink) $A_{e_\tau}(t)$ curve.

Note that the upper boundary $A_d(t)$ and $A_{e_\tau}(t)$ curves may cross and become underneath the lower boundary $D_{\min}(t)$ curve during part of the transmission period. No transmissions will take place during that part of the period due to insufficient energy. The part of the period is an infeasible solution region.

Algorithm 1 Proposed DST Algorithm

1: Input $\mathcal{A}$, $\mathcal{D}$, $\mathcal{E}$ and $\mathcal{T}$, set $n_{\text{offset}} = 0$, $r_i^* = l_i^* = 0, \forall i$.
2: **while** $n_{\text{offset}} < N$ **do**
3: Calculate r_n^a, r_n^d and r_n^e, $n = n_{\text{offset}} + 1, \ldots, N$;
4: $r^- = 0, r^+ = \infty, \tau^- = \tau^+ = 0$;
5: $\tau = N, \tilde{r} = r_N^a = r_N^d$;
6: **for** $n = n_{\text{offset}} + 1$ to N **do**
7: **if** $r^+ \geq \min\{r_n^a, r_n^e\}$ **then**
8: $r^+ = \min\{r_n^a, r_n^e\}$, $\tau^+ = n$;
9: **end if**
10: **if** $r^- \leq r_n^d$ **then**
11: $r^- = r_n^d$, $\tau^- = n$;
12: **end if**
13: **if** $r^- \geq r^+$ **then**
14: **if** $\tau^+ \geq \tau^-$ **then**
15: $\tau = \tau^-, \tilde{r} = r^-$;
16: **else**
17: $\tau = \tau^+, \tilde{r} = r^+$;
18: **end if**
19: break;
20: **end if**
21: **end for**
22: **for** $i = n_{\text{offset}} + 1$ to τ **do**
23: $r_i^* = \max\{r_{ee}, \tilde{r}\}$;
24: **end for**
25: **if** t_τ is the instant the data causality or deadline
26: constraint is met with equality **then**
27: find a feasible set of $\{l_i^*\}$ satisfying
28: $\sum_{i=n_{\text{offset}}+1}^{\tau} l_i^* = \sum_{i=n_{\text{offset}}+1}^{\tau} \frac{\tilde{r} L_i}{r_i^*}$
29: **else**
30: find a feasible set of $\{l_i^*\}$ satisfying
31: $\sum_{i=n_{\text{offset}}+1}^{\tau} l_i^* = \sum_{i=n_{\text{offset}}+1}^{\tau} \frac{[P(\tilde{r})+\rho] L_i}{P(r_i^*)+\rho}$
32: **end if**
33: update $(\mathcal{A}, \mathcal{D}, \mathcal{E}, \mathcal{T})$;
34: $n_{\text{offset}} = \tau$;
35: **end while**

B. Dynamic String Tautening Algorithm

Algorithm 1 summarizes the proposed off-line DST process in a structured way, which will play a key role in the practical on-line algorithm, as will be described in Section V. Denote $\mathcal{A} := \{A_0, A_1, \cdots, 0\}$, $\mathcal{D} := \{0, D_1, \cdots, D_N\}$, $\mathcal{E} := \{E_0, E_1, \cdots, 0\}$, and $\mathcal{T} := \{t_0, t_1, \cdots, t_N\}$. n_{offset} denotes the left end of the series of strings to be tautened. It is initially set to zero, and updated through the WHILE loop of Steps 2 to 35.

Steps 3 to 33 describe the operations specified in Rules 1–3 in Section IV-A. In Steps 3 to 21, the number of epochs since n_{offset}, during which the optimal transmit rate keeps unchanged, is identified by recursively updating and comparing r^+ (in Steps 7-9), the minimum of the rates determined by the upper boundary of the feasible region (i.e., r_n^a and r_n^e), and r^- (in Steps 10-12), the maximum of the rates determined by the lower boundary of the region (i.e., r_n^d), from $n = n_{\text{offset}} + 1$ until $r^- \geq r^+$ (in Steps 13-20). τ indicates the index of the time instant at which the string bends, i.e., the optimal transmit rate changes. In other words, Steps 3 to 21 determine every straight segment of the entire string generated by Rule 1 in every iteration. By iteratively running Steps 3 to 21, the string connecting $(0, 0)$ and the rightmost joint of the $A_d(t)$ and $D_{\min}(t)$ curves, which is specified in Rule 1, can be determined. As mentioned in (20), r_n^e satisfies $\sum_{i=n_{\text{offset}}+1}^{n}\{[P(r_n^e)+\rho]L_i\} = \sum_{i=n_{\text{offset}}}^{n-1} e_i$. It is unique and can be determined by a bisectional search per n, since $P(\cdot)$ is monotonically increasing. Likewise, r_n^a and r_n^d can be obtained by solving $\sum_{i=n_{\text{offset}}+1}^{n}(r_n^a L_i) = \sum_{i=n_{\text{offset}}}^{n-1} A_i$ and $\sum_{i=n_{\text{offset}}+1}^{n}(r_n^d L_i) = \sum_{i=n_{\text{offset}}+1}^{n} D_i$, respectively.

Steps 22 to 24 adjust the transmit rate to be no less than r_{ee}. Steps 25 to 33 summarize the operations that decide the durations associated with the optimal transmit rates determined above, as specified in Rule 2. Particularly, Steps 30 and 31 describe the case where the tentative $A_{e_\tau}(t)$ curve needs to be lifted and subsequently the duration of a transmission with r_{ee} is to be extended, as discussed earlier in Section IV-A.

As noted earlier in Section IV-A, the solution region of the optimal transmit schedule may be infeasible. The data arrival and EH processes are independent by nature. It is then possible that the transmitter runs out of energy when there are still deadline-approaching data in the buffer, i.e., D_i is too large to be supported by the available energy harvested and accumulated so far. In this case, the upper boundary curve can cross and go underneath the lower boundary $D_{\min}(t)$ curve, the problem becomes infeasible. No transmissions can be scheduled until new energy is harvested. Data with deadlines within the infeasible region are dropped.

The following theorem confirms the global optimality and efficiency of the proposed Algorithm 1.

Theorem 1. *Algorithm 1 can find the optimal transmission schedule for* (3) *when it is feasible.*

The theorem can be proved by first confirming the existence of a Lagrange multiplier vector $\boldsymbol{\Lambda}^*$, with which $\boldsymbol{r}^*$ and $\boldsymbol{l}^*$ satisfy the sufficient and necessary conditions (10)–(13), followed by showing that $(\boldsymbol{r^*}, \boldsymbol{l^*})$ ensures $l_i^* = L_i$ when $r_i^* > r_{ee}$ and $l_i^* \leq L_i$ when $r_i^* = r_{ee}$. In other words, $(\boldsymbol{r^*}, \boldsymbol{l^*})$ is a global optimum. A detailed proof of the theorem is provided in Appendix C.

We also confirm that Algorithm 1 has a complexity of $\mathcal{O}(N^2)$ in the worst case with regard to complexity. In that case, the optimal transmit rate changes at every instant, i.e., N optimal rates are to be calculated. Besides, to confirm the rate change at any instant, all the future instants after that instant need to be evaluated. This is because r^- remains less than r^+ until the last instant at which r^- becomes equal to or larger than r^+. As a result, at every instant t_n $(n = 0, 1, \cdots, N-1)$, the algorithm evaluates the future $(N-n)$ instants. It calculates the three rates r_i^a, r_i^e and r_i^d, compares $\min\{r_i^a, r_i^e\}$ with r^+ and compares r_i^d with r^-, and updates r^+ and r^- (as described in Steps 3 to 21), from $i = n+1$ all the way through $i = N$. The calculation required is $3\sum_{n=0}^{N-1}(N-n) = \frac{3}{2}(N^2+N)$.

In fact, the complexity of Algorithm 1 is much lower than $\mathcal{O}(N^2)$ in most cases. This is because the optimal transmit rate may keep unchanged across a number of instants; in other words, fewer optimal transmit rates need to be calculated. It is also because it often does not require all the future instants to be evaluated to get $r^- \geq r^+$. Fewer instants are evaluated to calculate an optimal transmit rate.

In contrast, the standard convex solvers designed for generality, such as the interior point methods, typically require matrix operations, high-order multiplications and repeated iterations. They have a polynomial complexity higher than $\mathcal{O}(N^3)$ [23]. Corroborated by our simulations, the CPU time for Algorithm 1 is less than 3.7% of that with the standard CVX program [5], as will be shown in Section VI.

It is worth mentioning that our proposed algorithm can be readily extended to a general time-varying channel. In that case, the time-invariant channel coefficient h will be replaced by h_i $(i = 1, \cdots, N)$, where h_i is the channel coefficient per epoch i. The extension of our algorithm can be done by tautening the "water-level" w_i, defined in (5), in the same way as we did on r_i, since in the optimal schedule w_i only changes at the instants where the data/energy causality or the deadline constraint is met with equality, as proved in Appendix B. Based on a "water-level" based DST approach, the optimal w_i^* can be determined per epoch i. Given w_i^*, the optimal transmit rate r_i^* can then be determined using (17). It is clear that for the time-varying case, the water-filling type power allocation will be resulted; i.e., with the same water-level w_i^*, higher power (and rate) is allocated for epoch with better channel quality. Interested readers can refer to our conference paper [20] for such a generalization.

The emphasis of the paper is on unreliable and insufficient power supply of EH systems, which is the dominant cause of compromised QoS. We have also pointed out that the EH rate is typically low (e.g., 10%) in practice. For these reasons, we assume that the capacity of battery is large enough to accommodate the harvested energy; i.e., battery capacity induced energy overflow is not considered in our formulation to facilitate elaboration of main ideas. The impact of the finite battery capacity on the optimality of the proposed schedule will be tested through simulations in Section VI. It will be justified that a battery capacity of 1500 mJ (recall that the capacity of a typical AAA Alkaline battery is 2700 J) is sufficient to render negligible optimality loss for the proposed approach.

V. On-line Extension of Dynamic String Tautening

We proceed to extend the proposed off-line DST algorithm to practical on-line applications where a-priori knowledge on data and energy arrivals is unavailable.

The extension is done as such that, at any time instant, we set the current instant as t_0, and set the future latest deadline instant of all the arrived data as t_N. The period between the two instants is T. We use (18), (19) and (20) to plot the future data causality and deadline curves, and the energy curve between t_0 and t_N. The transmit rates till the latest future instant can be optimized by conducting the proposed DST algorithm within the feasible solution region specified by the curves. Data will be transmitted with the optimal transmit rates, until a new arrival of data or energy.

At the instant of the new data/energy arrival, the data arrival, deadline, and energy curves will be updated by taking the instant as the initial instant. The optimal transmit rate will be recalculated for the instant and beyond. This process repeats, and automates the on-line transmit schedule generation, as summarized in Algorithm 2.

Algorithm 2 Proposed On-line Scheduling based on DST Algorithm

while The transmitter is powered on **do**
  if new data or energy arrives at the current instant **then**
    Set the current instant as t_0, and the instant of
    the future latest data deadline as t_N;
    Update $(\mathcal{A}, \mathcal{D}, \mathcal{E}, \mathcal{T})$;
    Run Algorithm 1 to update the transmit rates
    through t_N;
  end if
  Transmit the data with the updated transmit rates;
end while

Of course, the on-line extension may not be optimal. This is because the transmit rates, optimized for a future period of T without a-priori data/energy arrival knowledge during the period, may violate Lemma 2 in the case where data or energy does arrive during the period and new schedules are generated. In the other cases, no data or energy arrives during the period. The schedule generated at the beginning of the period will remain optimal till the end of the period. In this sense, the on-line DST algorithm provides a structured way to schedule future transmissions in practice.

VI. Numerical Results

In this section, simulations are carried out to evaluate our proposed DST algorithms, where we set $\rho = 30$ mW (unless otherwise specified) and $|h|^2 = 20$ dB during $[0, T]$. The data arrival process and the EH process are modelled as two independent Poisson processes. The average data arrival rate is 1 packet/sec, unless otherwise specified. The average EH rate ranges from 40 to 400 mJ/sec. For illustration simplicity, we set all the packets with the same delay requirement (i.e., the maximum delay allowed). It is noteworthy that our algorithms are general and applicable to other stochastic processes of data arrival and EH.

For comparison purpose, we use the MATLAB CVX toolbox to solve (3) for off-line transmit schedules, and to replace Algorithm 1 in Algorithm 2 for on-line transmit schedule generation. The CVX toolbox is based on the standard convex optimization solver – the interior point methods [5]. It is effective and has been extensively used to solve optimization

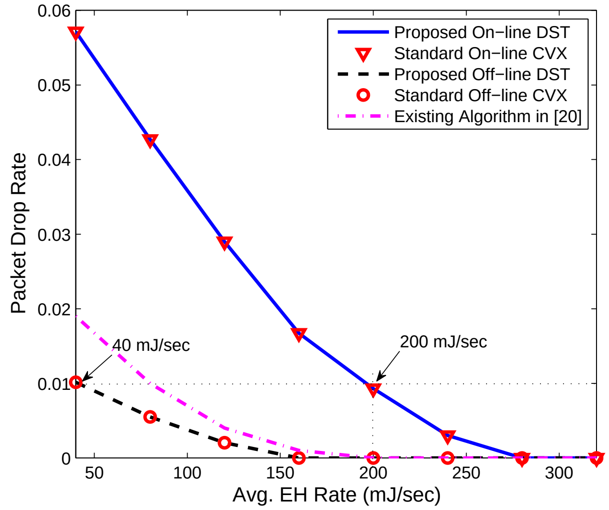

Fig. 2. Packet drop rate versus EH rate, where we assume the transmitter has unlimited battery capacity, the deadline is 2.5 seconds for every packet and the data arrival rate is 0.6 packet/sec.

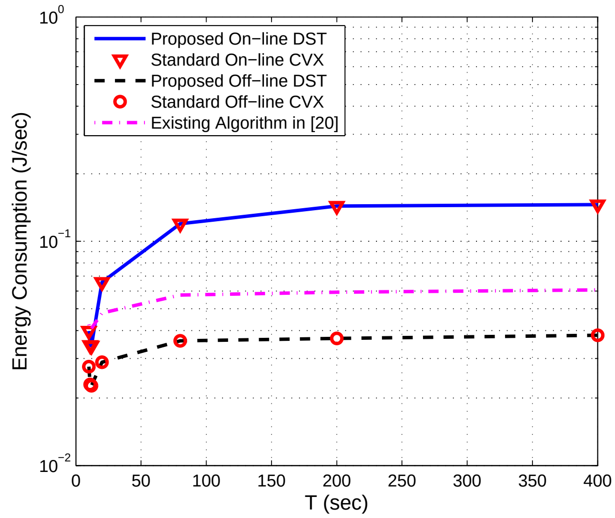

Fig. 3. Comparison of average energy consumption for the proposed algorithms, the existing algorithm developed in [20], and the standard CVX toolbox, where we assume the transmitter has unlimited battery capacity, the deadline is 2 seconds for every packet, the data arrival rate is 0.6 packet/sec and the EH rate is 400 mJ/sec.

problems with convex structures. Particularly, the CVX toolbox can produce the exactly same optimal schedules as our proposed algorithms, in the case where the energy consumed to generate transmit schedules is negligible as compared to the rest of the energy consumed on the circuit, such as baseband processing and radio generation. However, in practice, the energy for schedule generation is non-negligible, especially in short-distance wireless sensor networks. Given the complexity of $\mathcal{O}(N^3)$, the standard interior point methods would consume more energy, drain the battery faster, and incur higher packet losses than our proposed algorithms which only have a complexity of lower than $\mathcal{O}(N^2)$.

Figs. 2 and 3 validate the optimality of our proposed algorithms from the perspectives of PDR and total energy consumption, where the energy required to generate the optimal schedules is assumed to be negligible. The packet drop is caused by the expiration of the deadlines of some packets which are unsent due to insufficient energy. The optimality of the proposed algorithms is confirmed by comparing to the optimal results of the CVX toolbox, and revealing that the results of our algorithms coincide with those of the CVX toolbox.

In a sense, our proposed algorithm can minimize the infeasible region, by developing the most energy-efficient transmit schedules. In other words, it can minimize the number of packets dropped. This is because our algorithm can minimize the number of undelivered packets by the instant when the problem becomes infeasible. As a result, the energy requirement is minimized for the problem to become feasible again, which minimizes the duration of the infeasible region, as well as the packets dropped during the region.

As expected, the figures also show that on-line generation of transmit schedules can increase the PDR and the energy consumption, compared to the optimal schedules generated off-line. This is due to the unavailability of future knowledge on data and energy arrival in practice. As a result, the on-line transmit rates change more frequently than the optimal rates generated off-line. The energy consumption grows, as shown in Fig. 3. In turn, more packets are dropped, as shown in Fig. 2. In this sense, a higher EH rate is required for on-line algorithms to maintain a given PDR. Consider a PDR of 1%. The proposed on-line algorithm needs to increase the EH rate from 40 mJ/sec of the proposed off-line optimal scheme to 200 mJ/sec, as pointed out in Fig. 2.

Figs. 2 and 3 also reveal that the circuit power consumption can have significant impact on the optimal transmit schedules. The PDR and energy consumption of the off-line energy-efficient transmit schedule optimized under the assumption of negligible circuit power consumption are plotted, using the algorithm developed in [20]. It is shown that a significant loss of both the packet and energy would occur if the circuit power consumption is neglected. Our proposed algorithms, which take the circuit power consumption into account, are important, and have applications to practical circuits.

In practice, the energy consumed to generate transmit schedules is often non-negligible, due to the complexity involved. Fig. 4 plots the average CPU time required for the proposed algorithms in comparison to the CVX toolbox, where T ranges from 10 to 320 seconds, and the EH rate is 400 mJ/sec. It is shown that the proposed off-line and on-line algorithms, i.e., Algorithms 1 and 2, only require about 3.7% and 1.6% of the CPU time that the standard CVX toolbox requires for large T values, respectively. This is because our algorithms are specialized and directly construct the optimal solution for (3) based on the optimality conditions. Therefore, they are much more computationally efficient than the CVX toolbox, which is general and is designed to solve any convex optimization problems.

As noted earlier, the proposed Algorithm 1 has a worst-case complexity of $\mathcal{O}(N^2)$, whereas the general CVX toolbox has a complexity of $\mathcal{O}(N^3)$. On the other hand, a much larger gap

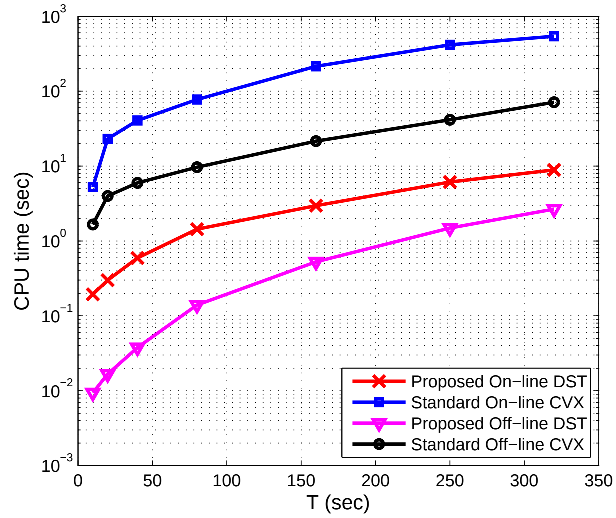

Fig. 4. Comparison of average CPU time for the proposed off-line and on-line algorithms, with the CVX toolbox.

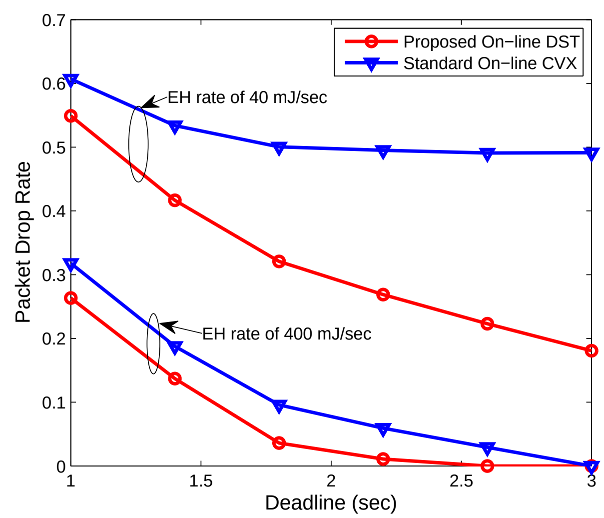

Fig. 5. Packet drop rate of the proposed Algorithm 2 and the on-line CVX program versus delay requirement, where we assume the transmitter has unlimited battery capacity and the data arrival rate is 1 packet/sec.

of complexity can be observed between Algorithm 1 and the CVX toolbox in Fig. 4. This confirms that Algorithm 1 has a significantly lower complexity in most cases than it has in the worst case, as discussed earlier in Section IV-B.

In light of Fig. 4, we proceed with a practical on-line scenario, where the energy for generating transmit schedules is non-negligible. Consider $\rho = \rho_1 + \rho_2$, where ρ_1 is the non-negligible energy consumption on schedule generation and ρ_2 is the rest of the energy consumed on the circuit. ρ_1 can differ between the proposed Algorithm 2 and the CVX program. We assume $\rho_1 = 15$ mW for Algorithm 2. The value of ρ_1 for the on-line CVX program depends on the ratio of the CPU time between the CVX program and Algorithm 2. The ratio can be obtained from Fig. 4. ρ_2 stays the same for both the approaches. We set $\rho_2 = 15$ mW.

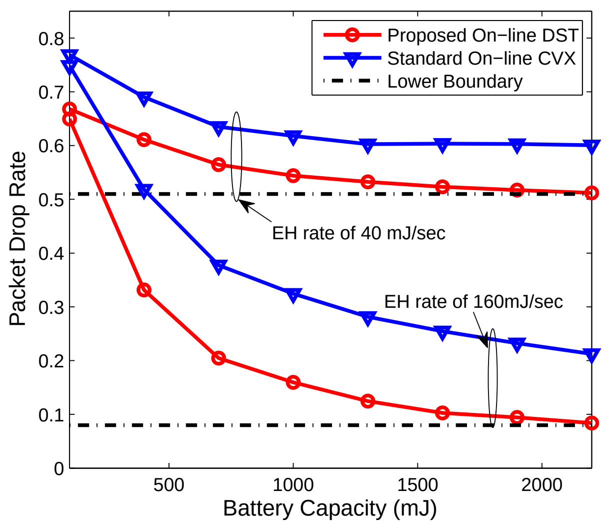

Fig. 6. Packet drop rate of the proposed Algorithm 2 and the on-line CVX program versus battery capacity, where the data arrival rate is 1 packet/sec and the deadline requirement is 2.5 seconds.

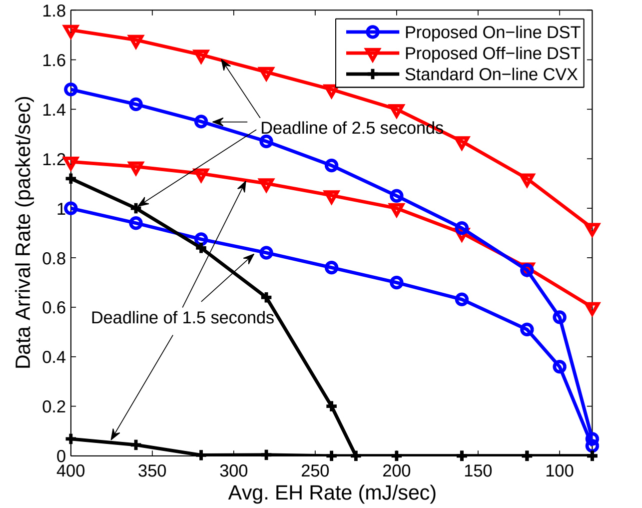

Fig. 7. EH rate versus packet arrival rate, where we assume the transmitter has unlimited battery capacity, the deadline is 2.5 seconds for every packet.

Fig. 5 compares the PDR of the proposed Algorithm 2 and the on-line CVX program with the growth of deadline, where the transmitter is assumed to have unlimited battery. As expected, the PDR decreases, as the deadline increases. It also decreases, as the EH rate increases. The reason for these is obvious, i.e., more available energy and/or looser data deadlines allow more packets to be delivered, hence reducing the PDR. In either case, we see that Algorithm 2 is better than the CVX program, given its superiority of substantially reduced energy requirement (as implied by Fig. 4).

As observed in Fig. 5, the reduced PDR of Algorithm 2 (compared to the CVX program) diminishes with the increasing deadline for large EH rates (e.g., 400 mJ/sec), while keeping growing for small EH rates (e.g., 40 mJ/sec). The reason for this is that the higher energy requirement of the CVX program makes the approach "saturate" at a smaller EH rate. In other words, the PDR stops decreasing further with the growth of deadline. It would not converge to zero, even without deadline (i.e., the deadline is infinite). The convergent/saturated PDR value can be easily obtained by first calculating the difference between the total energy harvested and the total energy consumed on the circuit, and then the number of packets that can be supported by the energy difference using r_{ee}.

Given the substantially low energy requirement, our proposed Algorithm 2 tolerates much smaller EH rates before saturating. Our algorithm also has much lower convergent PDR values. As shown in Fig. 5, the CVX program saturates with a convergent PDR of about 50%, when the EH rate is 40 mJ/sec. Meanwhile, Algorithm 2 is unsaturated, and it exhibits the obvious tendency of continuously decreasing.

Fig. 6 compares the PDR of the proposed Algorithm 2 and the standard on-line CVX program with the growth of the limited battery at the transmitter. The battery overflows, if the energy harvested and accumulated exceeds the battery capacity. As expected, we see that the PDR starts by decreasing with the growth of battery capacity at the transmitter, and then becomes flat when the battery is large and little energy is overflown. We also see that our proposed algorithm outperforms the standard CVX program with a consistent PDR reduction, across the entire spectrum of battery capacity, for a given EH rate. The consistent PDR reduction is due to the energy that our algorithm saves against the CVX program, and the saved energy is independent of the battery capacity.

The consistent PDR reduction is also enlarged when the EH rate increases; in other words, more energy can be saved with the increased EH rate. Specifically, the CVX program has bigger ρ and subsequently a smaller r_{ee} according to (16), compared to the proposed Algorithm 2. This increases the likelihood of transmitting data over an entire epoch with a less energy-efficient rate r_n^e or r_n^a, since the optimal rate is the largest of r_{ee} and those rates based on Lemma 1. The likelihood is further increased due to more and shorter epochs with the increased EH rate. The increased number of epochs, over which the energy is less efficiently utilized in the CVX program, results in the enlarged gap between Algorithm 2 and the CVX program. More energy is saved by the proposed Algorithm 2, and more packets can be sent using the saved energy under a larger EH rate.

Last but not least, we plot the trade-off between the data arrival rate and the EH rate in Fig. 7, where we set a fixed PDR of 10%. In addition to Algorithm 2 and the on-line CVX program, we also plot the proposed optimal off-line algorithm – Algorithm 1. In general, the proposed on-line algorithm, Algorithm 2, substantially surpasses the standard on-line CVX program. The effective on-line transmit region, which is the close region underneath every plotted curve, is significantly larger in Algorithm 2 than it is in the on-line CVX program. This is the result of the reduced complexity of Algorithm 2, and significantly more data or less energy can be supported in the proposed algorithm. The difference of sizes between the effective transmit regions of the two on-line approaches enlarges with the increased tightness of deadline.

VII. Conclusions

In this paper, we proposed the new DST algorithm to generate the optimal off-line transmit schedule for delay-limited traffic under non-negligible circuit power. Only consisting of a set of string tautening rules that we derived from the optimality conditions of the original problem, the proposed algorithm has a low complexity (i.e., $\mathcal{O}(N^2)$ in the worst case). We also extended the algorithm to generate energy-efficient transmit schedules on-the-fly. Simulation shows that our algorithm reduces the average complexity by almost two orders of magnitude, compared to general convex solvers. The effective transmit region can also be substantially enlarged by our algorithm. Significantly more data or less energy can be supported in the proposed algorithm. Building on this work, promising future directions include modeling more practical battery unit with finite capacity and energy leakage, accounting for charging/discharging loss, and developing low-complexity on-line schemes with analytical performance guarantees.

Appendix

A. Proof of Lemma 1

Define $\xi_{ee}(r) := \frac{P(r)+\rho}{r}$. Taking the first derivative of $\xi_{ee}(r)$, we have:

$$\frac{d\xi_{ee}(r)}{dr} = \frac{P'(r)r - (P(r)+\rho)}{r^2}. \tag{23}$$

Due to its "convex-over-linear" form, we can show that $\xi_{ee}(r)$ first decreases and then increases with r, and it reaches the minimum at r_{ee}. This implies:

$$\begin{cases} P'(r)r - (P(r)+\rho) < 0, & \text{if} \quad r < r_{ee}, \\ P'(r)r - (P(r)+\rho) = 0, & \text{if} \quad r = r_{ee}, \\ P'(r)r - (P(r)+\rho) > 0, & \text{if} \quad r > r_{ee}. \end{cases} \tag{24}$$

If we have an $r_i^* < r_{ee}$ when $l_i^* > 0$, it follows from (24) that $P'(r_i^*)r_i^* - (P(r_i^*)+\rho) < 0$. But when $P'(r_i^*)r_i^* - (P(r_i^*)+\rho) < 0$, (15) implies that $l_i^* = 0$, which leads to a contradiction. Hence, $r_i^* < r_{ee}$ is not allowed when $l_i^* > 0$.

When $r_i^* > r_{ee}$, we have $P'(r_i^*)r_i^* - (P(r_i^*)+\rho) > 0$ according to (24). This together with (15) then dictates $l_i^* = L_i$. In the case of $r_i^* = r_{ee}$, we have $P'(r_i^*)r_i^* - (P(r_i^*)+\rho) = 0$, so any $l_i^* \in [0, L_i]$ is a minimizer in (15).

B. Proof of Lemma 2

Clearly, $r_i^* = {P'}^{-1}(w_i)$ changes only when w_i changes its value. By the definition of w_i in (5), if $(\lambda_n^c)^*, (\lambda_n^d)^*, (\mu_n^c)^* = 0, \forall n = 1, \ldots, N-1$, then a constant $w = [(\lambda_N^d)^* - (\lambda_N^c)^*]/[1+(\mu_N^c)^*]$ will be used over all the epochs. We will have a change only when one of the Lagrange multipliers is positive for a certain $n \in [1, N-1]$, which occurs at the corresponding t_n. In addition, it follows from the complementary slackness conditions (11)-(13) that we have the corresponding constraints met with equality at such a t_n.

If the rate changes at t_n where $\sum_{i=1}^{n}(r_i^* l_i^*) = \sum_{i=0}^{n-1} A_i$, the corresponding $(\lambda_n^c)^* > 0$. For the epoch n, we have $w_n = \sum_{l=n}^{N}[(\lambda_l^d)^* - (\lambda_l^c)^*]/[1+\sum_{l=n}^{N}(\mu_l^c)^*]$. On the other hand, we have $w_{n+1} = \sum_{l=n+1}^{N}[(\lambda_l^d)^* - (\lambda_l^c)^*]/[1+\sum_{l=n+1}^{N}(\mu_l^c)^*]$ for the epoch $(n+1)$; thus, $w_{n+1} - w_n = (\lambda_n^c)^*/[1+\sum_{l=n+1}^{N}(\mu_l^c)^*] > 0$. We can conclude that the rate increases after this t_n as ${P'}^{-1}(w_i)$ is an increasing function of w_i.

If a change occurs at a certain t_n where $\sum_{i=1}^{n}(r_i^* l_i^*) = \sum_{i=1}^{n} D_i$, then $(\lambda_n^d)^* > 0$. We can similarly obtain that $w_{n+1} - w_n = -(\lambda_n^d)^*/[1+\sum_{l=n+1}^{N}(\mu_l^c)^*] < 0$, which indicates the rate decreases after this t_n.

If a change occurs at a certain t_n where $\sum_{i=1}^{n}[(P(r_i^*)+\rho)l_i^*] = \sum_{i=0}^{n-1} E_i$, then $(\mu_n^c)^* > 0$. We can derive that $1/w_n - 1/w_{n+1} = (\mu_n^c)^*/\sum_{l=n+1}^{N}[(\lambda_l^d)^* - (\lambda_l^c)^*] > 0$, which indicates the rate increases after this t_n.

C. Proof of Theorem 1

Given the rules in Algorithm 1, it can be shown that the rate-changing pattern in the transmit schedule $\mathcal{R} := (\boldsymbol{r^*}, \boldsymbol{l^*})$ produced by Algorithm 1 is consistent with the optimal structure revealed in Lemma 2 [20], i.e., (i) if the rate in use is first r and then changed to $\tilde{r}$ at t_τ where $\sum_{i=1}^{\tau}(r l_i^*) = \sum_{i=0}^{\tau-1} A_i$ or $\sum_{i=1}^{\tau}\{[P(r)+\rho]l_i^*\} = \sum_{i=0}^{\tau-1} E_i$, then we must have $\tilde{r} > r$; and (ii) if the rate r is changed at t_τ where $\sum_{i=1}^{\tau}(r l_i^*) = \sum_{i=1}^{\tau} D_i$, then we must have the next rate $\tilde{r} < r$.

Suppose that the rate changes M times in $\mathcal{R}$ yielded by Algorithm 1 at time instants $\{t_{\tau_1}, t_{\tau_2}, \ldots, t_{\tau_M}\}$. We divide the schedule into $M+1$ phases: rate $r_i^* = \check{r}_1$ over epochs $i \in [1, \tau_1]$, $r_i^* = \check{r}_2$ over epochs $i \in [\tau_1+1, \tau_2], \ldots, r_i^* = \check{r}_{M+1}$ over epochs $i \in [\tau_M+1, N]$. We can then construct a set of Lagrange multipliers $\boldsymbol{\Lambda^*} := \{(\lambda_n^c)^*, (\lambda_n^d)^*, (\mu_n^c)^*, n = 1, \ldots, N\}$ as follows:

For convenience, let Δ_1 denote $[P'(\check{r}_{m+1}) - P'(\check{r}_m)]$ and Δ_2 denote $[\frac{1}{P'(\check{r}_m)} - \frac{1}{P'(\check{r}_{m+1})}]$. For a certain τ_m, $\forall m = 1, \ldots, M$,

1) if $\sum_{i=1}^{\tau_m}(r_i^* l_i^*) = \sum_{i=0}^{\tau_m-1} A_i$, then
$$(\lambda_{\tau_m}^c)^* = \Delta_1 \cdot [1 + \sum_{l=\tau_m}^{N}(\mu_l^c)^*];$$
2) if $\sum_{i=1}^{\tau_m}(r_i^* l_i^*) = \sum_{i=1}^{\tau_m} D_i$, then
$$(\lambda_{\tau_m}^d)^* = -\Delta_1 \cdot [1 + \sum_{l=\tau_m}^{N}(\mu_l^c)^*];$$
3) if $\sum_{i=1}^{\tau_m}\{[P(r_i^*)+\rho]l_i^*\} = \sum_{i=0}^{\tau_m-1} E_i$, then
$$(\mu_{\tau_m}^c)^* = \Delta_2 \cdot \sum_{l=\tau_m}^{N}[(\lambda_l^d)^* - (\lambda_l^c)^*];$$

We have shown that the rate $\check{r}_{m+1} > \check{r}_m$ if the data or energy causality constraint is tight at t_{τ_m}, and $\check{r}_{m+1} < \check{r}_m$ if the deadline constraint is tight at t_{τ_m}. Recalling that $P'(r)$ is increasing in r, it readily follows that $(\lambda_{\tau_m}^c)^* > 0$, $(\lambda_{\tau_m}^d)^* > 0$, or $(\mu_{\tau_m}^c)^* > 0$, depending on which type of constraint is tight at t_{τ_m}. Besides, let $(\lambda_N^d)^* = P'(\check{r}_{M+1}) > 0$. Except these $M+1$ positive $(\lambda_N^d)^*$, $(\lambda_{\tau_m}^c)^*$, $(\lambda_{\tau_m}^d)^*$ and $(\mu_{\tau_m}^c)^*$, all other Lagrange multipliers in $\boldsymbol{\Lambda^*}$ are set to zero.

With such a $\mathbf{\Lambda}^*$, the complementary slackness conditions (11)-(13) clearly hold. Using such a $\mathbf{\Lambda}^*$ leads to $w_i := \sum_{n=i}^{N}[(\lambda_n^d)^* - (\lambda_n^c)^*]/[1 + \sum_{n=i}^{N}(\mu_n^c)^*] = P'(\check{r}_m), \forall i \in [\tau_{m-1}+1, \tau_m]$ (with $\tau_0 := 1$ and $\tau_{M+1} := N$). This implies that $r_i^* = \check{r}_m = [\log(|h|^2 w_i)]_+, \forall i \in [\tau_{m-1}+1, \tau_m]$. In addition, the construction of $\mathcal{R}$ ensures $l_i^* = L_i$ when $r_i^* = \check{r}_m > r_{ee}$, and computes a feasible set of $l_i^* \leq L_i$ when $r_i^* = \check{r}_m = r_{ee}$ in each phase m. This guarantees that each pair of (r_i^*, l_i^*) satisfies (10); thus, $(\boldsymbol{r}^*, \boldsymbol{l}^*)$ follows the optimal structure in Lemma 1.

References

[1] C. Valenta and G. Durgin, "Harvesting wireless power: Survey of energy-harvester conversion efficiency in far-field, wireless power transfer systems," *IEEE Microw. Mag.*, vol. 15, no. 4, pp. 108–120, May 2014.

[2] D. Gunduz, K. Stamatiou, N. Michelusi, and M. Zorzi, "Designing intelligent energy harvesting communication systems," *IEEE Commun. Mag.*, vol. 52, no. 1, pp. 210–216, Jan. 2014.

[3] W. Ni, R. P. Liu, J. Biswas, X. Wang, I. B. Collings, and S. Jha, "Multiuser MIMO scheduling for mobile video applications," *IEEE Trans. Wireless Commun.*, vol. 13, no. 10, pp. 5382–5395, Oct. 2014.

[4] C. Isheden, Z. Chong, E. Jorswieck, and G. Fettweis, "Framework for link-level energy efficiency optimization with informed transmitter," *IEEE Trans. Wireless Commun.*, vol. 11, no. 8, pp. 2946–2957, Aug. 2012.

[5] M. Grant and S. Boyd, *CVX: Matlab software for disciplined convex programming*. http://cvxr.com/cvx/, Mar. 2015.

[6] J. Yang and S. Ulukus, "Optimal packet scheduling in an energy harvesting communication system," *IEEE Trans. Commun.*, vol. 60, no. 1, pp. 220–230, Jan. 2012.

[7] K. Tutuncuoglu and A. Yener, "Optimum transmission policies for battery limited energy harvesting nodes," *IEEE Trans. Wireless Commun.*, vol. 11, no. 3, pp. 1180–1189, Mar. 2012.

[8] O. Ozel, K. Tutuncuoglu, J. Yang, S. Ulukus, and A. Yener, "Transmission with energy harvesting nodes in fading wireless channels: Optimal policies," *IEEE J. Sel. Areas Commun.*, vol. 29, no. 8, pp. 1732–1743, 2011.

[9] J. Xu and R. Zhang, "Throughput optimal policies for energy harvesting wireless transmitters with non-ideal circuit power," *IEEE J. Sel. Areas Commun.*, vol. 32, no. 2, pp. 322–332, Feb. 2014.

[10] Q. Bai, J. Li, and J. A. Nossek, "Throughput maximizing transmission strategy of energy harvesting nodes," in *Proc. IWCLD*, 2011, pp. 1–5.

[11] O. Orhan, D. Gunduz, and E. Erkip, "Throughput maximization for an energy harvesting communication system with processing cost," in *Proc. ITW*, 2012, pp. 84–88.

[12] M. Gregori and M. Payaro, "On the optimal resource allocation for a wireless energy harvesting node considering the circuitry power consumption," *IEEE Trans. Wireless Commun.*, vol. 13, no. 11, pp. 5968–5984, Nov. 2014.

[13] Z. Ding, S. Perlaza, I. Esnaola, and H. Poor, "Power allocation strategies in energy harvesting wireless cooperative networks," *IEEE Trans. Wireless Commun.*, vol. 13, no. 2, pp. 846–860, Feb. 2014.

[14] X. Wang and Z. Li, "Energy-efficient transmissions of bursty data packets with strict deadlines over time-varying wireless channels," *IEEE Trans. Wireless Commun.*, vol. 12, no. 5, pp. 2533–2543, May 2013.

[15] Z. Nan, X. Wang, and W. Ni, "Energy-efficient transmission of delay-limited bursty data packets under non-ideal circuit power consumption," in *Proc. of ICC*, 2014, pp. 4957–4962.

[16] G. Miao, N. Himayat, and G. Y. Li, "Energy-efficient link adaptation in frequency-selective channels," *IEEE Trans. Commun.*, vol. 58, no. 2, pp. 545–554, Feb. 2010.

[17] M. A. Zafer and E. Modiano, "A calculus approach to minimum energy transmission policies with quality of service guarantees," in *Proc. INFOCOM*, vol. 1, 2005, pp. 548–559.

[18] P. Youssef-Massaad, L. Zheng, and M. Mdard, "Bursty transmission and glue pouring: on wireless channels with overhead costs," *IEEE Trans. Wireless Commun.*, vol. 7, no. 12, pp. 5188–5194, Dec. 2008.

[19] D. Shuman, M. Liu, and O. Wu, "Energy-efficient transmission scheduling with strict underflow constraints," *IEEE Trans. Inf. Theory*, vol. 57, no. 3, pp. 1344–1367, Mar. 2011.

[20] X. Chen, X. Wang, and Y. Sun, "Energy-harvesting powered transmissions of bursty data packets with strict deadlines," in *Proc. of ICC*, 2014, pp. 4060–4065.

[21] X. Chen, X. Wang, and X. Zhou, "Energy-harvesting powered transmissions of delay-limited data packets," in *Proc. Globecom*, 2014.

[22] X. Wang and G. B. Giannakis, "Resource allocation for wireless multiuser OFDM networks," *IEEE Trans. Inf. Theory*, vol. 57, no. 7, pp. 4359–4372, July 2011.

[23] S. Boyd and L. Vandenberghe, *Convex Optimization*. Cambridge University Press, 2004.

PLACE PHOTO HERE

Xiaojing Chen received the B.E. degree in Communication Engineering from Fudan University, China in 2013. Currently she is working toward her Ph.D. degree in Fudan University. Her research interests include wireless resource allocation, energy-efficient communications and stochastic network optimization.

PLACE PHOTO HERE

Wei Ni (M'09-SM'15) received the B.E. and Ph.D. degrees in Electronic Engineering from Fudan University, Shanghai, China, in 2000 and 2005, respectively. Currently he is a Senior Scientist with CSIRO, Australia. He also holds adjunct positions with Macquarie University (MQ), Sydney, and the University of Technology, Sydney (UTS). Prior to this he was a Research Scientist and Deputy Project Manager at the Bell Labs R&I Center, Alcatel/Alcatel-Lucent (2005-2008), and a Senior Researcher at Devices R&D, Nokia (2008-2009). His research interests include radio resource management, software-defined networking (SDN), network security, and multiuser MIMO.

Dr Ni serves as Editor for Hindawi Journal of Engineering since 2012, secretary of IEEE NSW VTS Chapter since 2015, PHY Track Co-chair for IEEE VTC-Spring 2016, and Publication Chair for BodyNet 2015. He also served as Student Travel Grant Chair for WPMC 2014, a Program Committee Member of CHINACOM 2014, a TPC member of IEEE ICC14 workshop on body area networks, ICCC15, EICE14, and WCNC10.

PLACE PHOTO HERE

Xin Wang (SM'09) received the B.Sc. degree and the M.Sc. degree from Fudan University, Shanghai, China, in 1997 and 2000, respectively, and the Ph.D. degree from Auburn University, Auburn, AL, in 2004, all in electrical engineering.

From September 2004 to August 2006, he was a Postdoctoral Research Associate with the Department of Electrical and Computer Engineering, University of Minnesota, Minneapolis. In August 2006, he joined the Department of Computer & Electrical Engineering and Computer Science, Florida Atlantic University, Boca Raton, as an Assistant Professor, and then an Associate Professor from August 2010. He is now a Professor with the Department of Communication Science and Engineering, Fudan University, China. His research interests include stochastic network optimization, energy-efficient communications, cross-layer design, and signal processing for communications. He is an Associate Editor for the IEEE Transactions on Signal Processing, and an Editor for the IEEE Transactions on Vehicular Technology. He was an Associate Editor for the IEEE Signal Processing Letters.

PLACE PHOTO HERE

Yichuang Sun (M'90-SM'99) received the B.Sc. and M.Sc. degrees from Dalian Maritime University, Dalian, China, in 1982 and 1985, respectively, and the Ph.D. degree from the University of York, York, U.K., in 1996, all in communications and electronics engineering. He is currently a Professor with the School of Engineering and Technology of the University of Hertfordshire, UK. His research interests are in the areas of wireless and mobile communications and RF and analog circuits. He has published over 280 papers and contributed nine chapters in edited books. He has also published four text and research books: Continuous-time Active Filter Design, CRC Press, USA, Design of High frequency Integrated Analogue Filters, IEE/IET Press, UK, Wireless Communication Circuits and Systems, IET Press, and Test and Diagnosis of Analogue, Mixed-signal and RF Integrated Circuits - the Systems on Chip Approach, IET Press.

He was a Series Editor of IEE Circuits, Devices and Systems Book Series. He was Associate Editor of IEEE Transactions on Circuits and Systems-I in 2010-2011 and serves the journal as Associate Editor again in 2016-2017. He is Editor of ETRI Journal and Journal of Semiconductors. He has been lead or sole Guest Editor of seven IEEE and IEE/IET journal special issues which include MIMO Wireless and Mobile Communications published in IEE Proceedings: Communications, 2006, Advanced Signal Processing for Wireless and Mobile Communications in IET Signal Processing, 2009, Cooperative Wireless and Mobile Communications in IET Communications, 2013, and Software-Defined Radio Transceivers and Circuits for 5G Wireless Communications in IEEE Transactions on Circuits and Systems-II, 2016. He has also been widely involved in various IEEE technical committee and international conference activities.